Video Article

Protocol of Electrochemical Test and Characterization of Aprotic Li-O_2 Battery

Xiangyi Luo[1], Tianpin Wu[2], Jun Lu[1], Khalil Amine[1]

[1]Chemistry Sciences and Engineering Division, Argonne National Laboratory

[2]X-ray Science Division, Advanced Photon Sources, Argonne National Laboratory

Correspondence to: Jun Lu at junlu@anl.gov, Khalil Amine at amine@anl.gov

URL: https://www.jove.com/video/53740
DOI: doi:10.3791/53740

Keywords: Engineering, Issue 113, aprotic Li-O_2 battery, porous cathode, aprotic electrolyte, lithium anode, chemical engineering, electrochemistry, characterization

Date Published: 7/12/2016

Citation: Luo, X., Wu, T., Lu, J., Amine, K. Protocol of Electrochemical Test and Characterization of Aprotic Li-O_2 Battery. *J. Vis. Exp.* (113), e53740, doi:10.3791/53740 (2016).

Abstract

We demonstrate a method for electrochemical testing of an aprotic Li-O_2 battery. An aprotic Li-O_2 battery is made of a Li-metal anode, an aprotic electrolyte, and an O_2-breathing cathode. The aprotic electrolyte is a solution of lithium salt with aprotic solvent; and porous carbon is commonly used as the cathode substrate. To improve the performance, an electrocatalyst is deposited onto the porous carbon substrate by certain deposition methods, such as atomic layer deposition (ALD) and wet-chemistry reaction. The as-prepared cathode materials are characterized by scanning electron microscopy (SEM), transmission electron microscopy (TEM), and X-ray absorption near edge structure (XANES). A Swagelok-type cell, sealed in a glass chamber filled with pure O_2, is used for the electrochemical test on a battery test system. The cells are tested under either capacity-controlled mode or voltage controlled mode. The reaction products are investigated by electron microscopy, X-ray diffraction (XRD), X-ray photoelectron spectroscopy (XPS), attenuated total reflection Fourier transform infrared (ATR-FTIR) spectroscopy, and Raman spectroscopy to study the possible pathway of oxygen reduction reaction (ORR) and oxygen evolution reaction (OER). This protocol demonstrates a systematic and efficient arrangement of routine tests of the aprotic Li-O_2 battery, including the electrochemical test and characterization of battery materials.

Video Link

The video component of this article can be found at https://www.jove.com/video/53740/

Introduction

In 1996, Abraham and Jiang[1] reported the first reversible non-aqueous Li-O_2 battery consisting of a porous carbon cathode, an organic electrolyte, and a Li-metal anode. Since then, due to its extremely high theoretical energy density exceeding that of any other existing energy storage systems, the Li-O_2 battery, which induces a current flow by the oxidation of lithium at the anode and the reduction of oxygen at the cathode (overall reaction $Li^+ + O_2 + e^- \leftrightarrow Li_2O_2$), has received significant interest recently.[1-8]

A cathode material with the following requirements would be able to cater for the needs of high performance of Li-O_2 battery: (1) fast oxygen diffusion; (2) good electric and ionic conductivity; (3) high specific surface area; and (4) stability. Both the surface area and porosity of the cathode are critical for the electrochemical performance of Li-O_2 batteries.[9-12] The porous structure allows the deposition of solid discharge products generated from the reaction of Li cations with O_2; and larger surface areas provide more active sites to accommodate electrocatalytic particles that accelerate the electrochemical reactions. Such electrocatalysts are added to the cathode material by certain deposition methods, which provide strong adhesion to the substrate and good control of the catalyst particles, with preservation of the original porous surface structure of the substrate.[13-17] The as-prepared materials are tested in Swagelok-type cells as the cathode of aprotic Li-O_2 battery. However, the performance of the cell not only depends on the nature of cathode materials, but also on the type of the aprotic electrolyte[18-22] and Li-metal anode.[23-26] More influences include the amount and concentration of the materials and the procedure used in the charge/discharge tests. Proper conditions and protocols would optimize and improve the overall performance of battery materials.

In addition to the results of the electrochemical test, the battery performance can be also evaluated by characterizing the pristine materials and the reaction products.[27-33] Scanning electron microscopy (SEM) is used to investigate the surface microstructure of the cathode material and the morphology evolution of the discharge products. Transmission electron microscopy (TEM), X-ray absorption near edge structure (XANES), and X-ray photoelectron spectroscopy (XPS) can be used to determine the ultrastructure, chemical state, and component of elements, especially for that of catalyst nanoparticles. High-energy X-ray diffraction (XRD) is used for directly identifying the crystalline discharge products. Possible electrolyte decomposition can be determined by attenuated total reflection Fourier transform infrared (ATR-FTIR) and Raman spectra.

This article is a protocol that demonstrates a systematic and efficient arrangement of routine tests of the aprotic Li-O_2 battery, including the preparation of battery materials and accessories, the electrochemical performance test, and characterization of pristine materials and reaction products. The detailed video protocol is intended to help new practitioners in the field avoid many common pitfalls associated with the performance testing and characterization of Li-O_2 batteries.

Protocol

Please consult all relevant Material Safety Data Sheets (MSDS) before use. Several of the chemicals used in these syntheses are acutely toxic and carcinogenic. Nanomaterials may have additional hazards compared to their bulk counterpart. Please use all appropriate safety practices when performing a nanocrystal reaction including the use of engineering controls (fume hood, glovebox) and personal protective equipment (safety glasses, gloves, lab coat, full length pants, closed-toe shoes). Portions of the following procedures involve standard air-free handling techniques.

1. Synthesis of Cathode Materials

Note: Cathode materials can be synthesized by either atomic layer deposition or wet chemistry reaction.

1. **Atomic Layer Deposition (ALD)**
    1. Disperse 5 g of porous carbon in 100 ml 1 M $KMnO_4$ solution under magnetic stirring for 12 hr.
    2. Spread 100 mg of the oxidized carbon powder onto a stainless steel tray of the ALD instrument, and clamp a stainless steel mesh cover over the tray.
    3. Hold the carbon powder in the tray at 200 °C under continuous flow of 300 sccm ultra-high-purity nitrogen carrier gas at 1 Torr pressure for 30 min.
    4. Treat the carbon powder with a complete ALD cycle as follows.
    Note: Take Pd nanoparticles as an example of the electrocatalysts in this protocol. Reagents can be changed according to specific requirements. All reagents are used as-received without any further purification.
        1. Expose the carbon substrate (100 mg) to palladium hexafluoroacetylacetonate ($Pd(hfac)_2$, 99.9%) at 200 °C for 100 min.
        2. Purge the tray with continuous flow of 300 sccm ultra-high-purity nitrogen carrier gas at 1 Torr pressure for 300 min.
        3. Expose the carbon substrate to formalin (HCHO 37 wt. % in H_2O) at 200 °C for 100 min.
        4. Purge the tray with continuous flow of 300 sccm ultra-high-purity nitrogen carrier gas at 1 Torr pressure for 300 min.
    5. Repeat ALD cycle as necessary. Usually 3-10 repetitions.
2. **Wet-chemistry Reaction**
Note: Take Fe nanoparticles as an example of the electrocatalyst in this protocol. Reagents can be changed according to specific requirements. All reagents are used as-received without any further purification.
    1. Disperse 5 g of porous carbon in 100 ml 1 M $KMnO_4$ solution under magnetic stirring for 12 hr.
    2. Wash the oxidized carbon with deionized water.
    3. Filter the washed carbon with a filter flask fitted with a glass fiber, and then dry it in an oven at 110 °C for 12 hr.
    4. Disperse the dried carbon in 100 ml deionized water, then add 1 g of $FeCl_3$ under magnetic stirring.
    5. Adjust the pH value to about 9, using 1 M NaOH solution.
    6. Stir the resulting slurry for 5 hr, and then filter the slurry with a filter flask fitted with a glass fiber.
    7. Wash the product with deionized water and ethanol. Then dry it in an oven at 110 °C for overnight.
    8. Heat-treat the product at 450 °C with continuous flow of H_2/Ar mixture (4% H_2) in a quartz tube furnace. Use a flow rate of 100 ml/min for 5 hr.

2. Preparation of Electrodes and Electrolyte

1. **Cathode**
    1. Mix the as-prepared cathode material and binder poly(vinylidene fluoride) (PVDF) in a 4:1 weight ratio.
    Note: The total of the mixture depends on the amount of the cathodes. The loading of cathode material on each piece is in the range of 0.1-1 mg.
    2. Add 1-methyl-2-pyrrolidinone (NMP) to the mixture, and stir well to make an even-textured slurry. Add NMP at about three times the weight of the mixture.
    3. Coat the slurry onto carbon paper by a doctor blade with a thickness around 100 μm.
    4. Dry the laminate in a vacuum oven at 100 °C for overnight.
    5. Punch the laminate into disks with a hole puncher to a diameter of 7/16 inches, and weigh it.
2. **Aprotic Electrolyte**
    1. Dry lithium trifluoromethanesulfonate ($LiCF_3SO_3$) in a vacuum oven at 100 °C for overnight.
    2. Add dried $LiCF_3SO_3$ in tetraethylene glycol dimethyl ether (TEGDME; H_2O ~ 10 ppm) with a concentration of 1 mol/L, then stir the solution with magnetic stirring until the salt is dissolved.
    3. Keep the electrolyte in a glovebox filled with Ar.
3. **Anode**
    1. Punch the lithium foil/chips into disks with a hole puncher to a diameter of 7/16 inches.

3. Electrochemical Testing

1. **Assembly of Swagelok Cell**

Note: All the steps of the assembly are operated in a glovebox filled with Ar, except 3.1.9.

1. Assemble the Swagelok set as shown in **Figure 1a**. Tighten the anode end, and loosen the cathode end.
2. Put a piece of lithium metal chip (diameter 7/16 inches) on the top of the stainless steel rod of the anode end.
3. Put a piece of glass fiber separator (diameter 1/2 inches) on the top of the lithium metal anode.
4. Add 5-7 drops of electrolyte to fully wet the glass fiber separator. Gently press the separator to remove bubbles.
5. Put a piece of cathode on the top of the wetted separator, with the active material facing the anode.
6. Cover the cathode with a piece of aluminum mesh (diameter 7/16 inches).
7. Press the above mentioned layers with the aluminum tube, then tighten the cathode end.
8. Seal the whole Swagelok cell in a glass chamber, and fix the chamber with a clamp, as shown in **Figure 1**.
9. Take the whole cell out of glovebox. Connect the glass chamber to an ultra-high-purity oxygen tank, and purge it with continuous oxygen flow at 1 atm pressure for 30 min.

2. **Battery Performance Testing**
   1. Set a thermostat to 25 °C.
   2. Put cells and electrodes (electronic clips connected to the equipment by a cable) into the thermostat, and fix them.
   3. Clip the cathode and anode on glass chamber with corresponding electronic clips.
   4. Open the operating software of the battery test system, and select the channel connected with the cable.
   5. Set a procedure of the electrochemical testing.
      Note: Set the current density of 100 mA/$g_{\text{active material}}$, and voltage range of 2.2-4.5 V.
      1. Set the discharge cut-off voltage of 2.2 V for discharge test.
      2. Set the discharge/charge step-time of 5 or 10 hr for capacity-controlled cycling test.
      3. Set the discharge cut-off voltage of 2.2 V and charge cut-off voltage of 4.5 V for voltage-controlled cycling test.
   6. Run the procedure by clicking the "run" button on the software interface.

3. **Disassembly and cleaning of the cell**
   1. Disassemble cells in a glovebox.
   2. Keep the electrodes in glass vials for the following characterizations. Transfer other cell parts out of the glovebox.
   3. Put the Swagelok parts, stainless steel rods, aluminum tubes, and aluminum meshes in acetone solution (~ 20%) or deionized water in a beaker, and clean them with ultrasonication for 15-30 min.
   4. Dry the parts and glass chambers in a thermostat set to 60-80 °C.

4. Preparation of Characterization Specimens

Note: Specimens are prepared in a hood (for as-prepared materials) or a glovebox filled with Ar (for air-sensitive specimens).

1. **Specimens for SEM and XPS**
   1. Stick a carbon tape on the sample stage. The carbon tape can be as large as the sample stage, or as small as the specimen piece.
   2. Cut a piece of specimen about 5 mm^2, and stick it on the carbon tape.
      Note: The specimen can be any non-magnetic samples. For the specimens after electrochemical tests, wash them with the electrolyte solvent before stick to the carbon tape.
   3. Seal the air-sensitive specimens in a Mason jar before measurement.
   4. Operate the SEM[34-36] or XPS[37,38] according to the manufacturer's instructions.

2. **Specimens for TEM**
   1. Mill 1 mg of the sample powder.
      Note: For electrode specimens, scrape the active materials off carbon paper before milling.
   2. Load the sample powder onto a copper grid, and remove the loose powder.
   3. Load the copper grid to the sample holder of TEM.
      Note: Get this step done as fast as possible for air-sensitive samples.
   4. Perform TEM.[39-41]

3. **Specimens for High-energy XRD**
   1. **Powder specimens**
      1. Seal one end of a polyimide tubing by clay or glue.
      2. Load the powder into the tubing.
      3. Seal the other end of the tubing.
   2. **Disk specimens**
      Note: To measure the active materials on electrode, another option is to scrape them off carbon paper and follow step 4.3.1.
      1. Seal the sample pieces with a piece of polyamide tape. Seal by putting the samples in the middle of one piece of tape, and covering them with another piece of tape.
         Note: For the specimens after electrochemical tests, wash them with the electrolyte solvent before sealing.
   3. Operate the high-energy XRD[42-44] in Advanced Photon Sources in Argonne National Laboratory.

4. **Specimens for XANES**
   1. **Powder samples**
      1. Dilute the samples if the concentration of the measured elements is high, using either boron nitride (BN) or carbon black as the dilute agent. Here, dilute to 3-5 wt. %.

2. Press the powder into disk with the diameter of 7 mm and the thickness of around 1 mm, using a KBr Press Kit and 7 mm Die Set.
3. Seal the disk with window film.

2. **Disk specimens**
   1. Seal the specimen with window film.

3. Operate the high-energy XANES[45-47] in Advanced Photon Sources in Argonne National Laboratory.

5. **Specimens for ATR-FTIR**
   1. Clean the diamond attenuated total reflection (ATR) unit before and after measurement.
   2. Put specimens on the diamond unit for all samples interested.
   3. Perform ATR-FTIR spectrometry.[48,49]

6. **Specimens for Raman Spectra**
   1. Put the specimen on a flat board (glass, stainless steel, *etc.*).
   2. Cover the specimen with a cover slide.
   3. Seal the set for air-sensitive samples.
   4. Perform Raman spectrometry.[50,51]

Representative Results

Figure 1a shows the setup of the Swagelok-type cell of the Li-O_2 battery test. A piece of lithium film is placed on a stainless steel rod at the anode end. The porous cathode is open to pure O_2 through an aluminum tube. Glass fiber is used as a separator and an absorber of aprotic electrolyte; and Al-mesh is used as a current-collector. The whole Swagelok-type cell is sealed in a glass chamber filled with ultra-high purity oxygen. For in-depth study, multiple characterization methods are applied to examine the battery system, including the as-prepared electrode materials and the reaction products. SEM and TEM images present the microstructure of the samples. SEM images of the carbon powder before (**Figure 1c**) and after (**Figure 1d**) the catalyst loading demonstrate a well preservation of the porous surface structure. TEM images (**Figure 1e**) shows the electrocatalyst nanoparticles uniformly distribute on the carbon substrate; and well crystallized nanoparticles are shown in the high-resolution TEM image in **Figure 1f**. Although electron microscopy images show the detail morphology and structure of the electrocatalysts, other X-ray based characterization techniques can provide more information on their chemical composition and valance state. As shown in **Figure 1b**,[13] XANES spectra, which are applied to determine the valence states, show that the electrocatalyst nanoparticles are partly oxidized due to the preparation of cathodes in air.

As-prepared cathode materials are tested in Swagelok-type cells in a voltage window of 2.2-4.5 V (*vs* Li^+/Li). Typical voltage profiles for discharge and discharge-charge cycles are shown in **Figure 2a** and **b**. With the presence of the electrocatalyst loaded by ALD, the discharge specific capacity increased to over 4,000 mAh/g when the cell is discharged to 2.2 V, compared to that of the cathode without the electrocatalysts (905 mAh/g). The charge potential reduced to 3.4 V when the cell capacity is controlled at 500 mAh/g (**Figure 2b**), which are significant improvements comparing with charge potential of 4 V (**Figure 2b**) for bare carbon cathodes. To better evaluate the battery performance and understand the electrochemical reaction mechanism, the samples at different discharge/charge stages are subjected to the characterization using multiple advanced techniques. In the SEM image of discharged cathode as shown in **Figure 2c**, the discharge products have the toroidal shape, which are widely accepted as the primary morphology of Li_2O_2 in a Li-O_2 cell.[15,52] XRD pattern is used as a direct evidence to identify crystalline products. There are only peaks of Li_2O_2 and carbon in the XRD pattern of the discharged cathode (**Figure 2d**), suggesting that the side reactions are minimized in the cell.

XPS and Raman spectra are used to identify the surface composition on electrodes at different charge/discharge status. According to the XPS spectra (**Figure 3a**), Li_2O_2 and LiOH form on the cathode surface after discharging; and by charging, Li_2O_2 is reduced but the irreversible product LiOH remains on the surface. A slight amount of LiO_2, an intermediate product of the one-electron transfer ORR, is detected by Raman spectroscopy (**Figure 3b**). LiO_2 is metastable due to its easy disproportionation, which makes only detected by surface-sensitive characterization technique like Raman spectroscopy. The vibration signal of O-H and C=O bond in the FT-IR spectra (**Figure 3c** and **d**) indicates the presence of the ether electrolyte as well as other hydroxide, carbonate, or carbonyl species on the surface of Li anode or the glass fiber separator, which form in the side reactions such as the electrolyte decomposition and oxygen crossover effect.

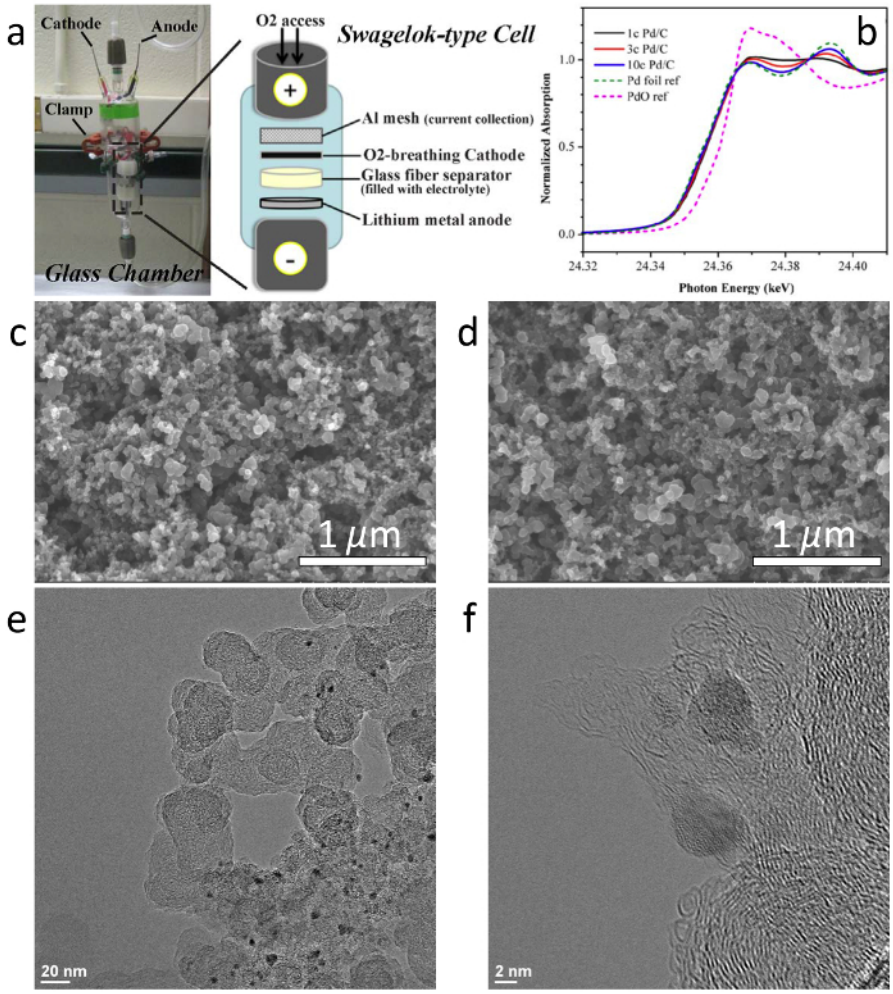

Figure 1. Swagelok-type cell and as-prepared materials. (**a**) Schematics of a Swagelok-type cell sealed in a glass chamber. (**b**) Pd K-edge XANES spectra of the as-prepared cathode material, reprinted from ref. 13. (**c**, **d**) SEM images of the carbon powder before and after electrocatalyst loading, respectively. (**e**, **f**) TEM and HRTEM images of the carbon powder with electrocatalyst, respectively. Please click here to view a larger version of this figure.

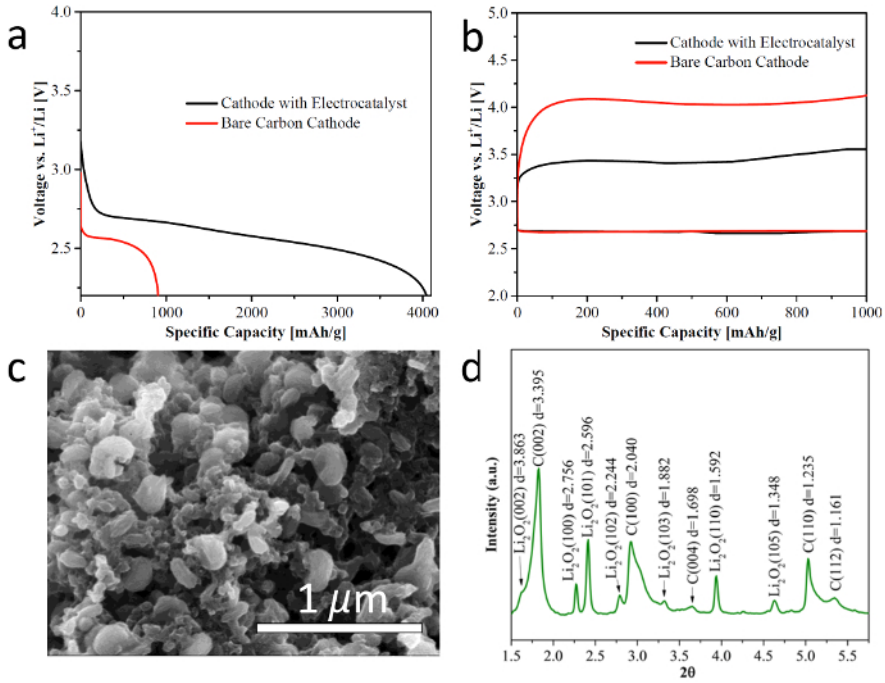

Figure 2. Voltage Profiles of the discharge/charge process and characterization of the discharged cathodes. (**a**, **b**) Voltage profile of a discharge to 2.2 V and a capacity-controlled discharge-charge cycle, respectively. (**c**, **d**) SEM image and high-energy XRD pattern of the cathode discharged in Swagelok-type Li-O_2 battery, respectively. Please click here to view a larger version of this figure.

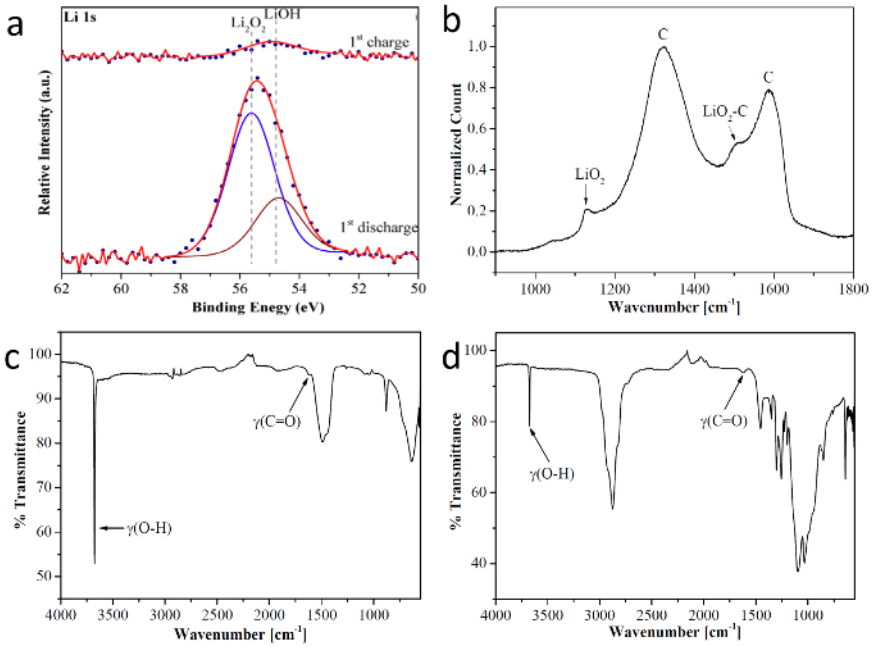

Figure 3. Characterization results. (**a**) XPS spectra of Li 1s peaks at different charge/ discharge status, reprinted from ref. 13. (**b**) Raman spectra of the carbon cathodes discharged to 2.5 V. (**c**, **d**) FTIR spectra of the anode and separator after discharge-charge cycles, respectively. Please click here to view a larger version of this figure.

Discussion

Considering the sensitivity of Li-O_2 battery system to air, especially CO_2 and moisture, lots of steps in the protocol are necessary in order to reduce the interferents and to avoid side reactions. For example, the Swagelok-type cell is assembled in a glovebox filled with Ar with O_2 < 0.5 ppm and H_2O < 0.5 ppm; and all the cathode materials, electrolyte solvent and salt, glass fiber, Swagelok parts, and the glass chambers are dried before assembly to reduce the moisture contamination. The anode end is a stainless steel rod in order to avoid the direct contact between lithium metal and O_2 and to protect the lithium anode. The whole Swagelok setup is placed into a pure-oxygen-filled glass chamber which

guarantees a leak-proof container by sealing with O-ring and vacuum greases. Moreover, Al-mesh, the current-collector, can help to protect the brittle carbon cathode.

The electrochemical test demonstrate that the as-prepared cathode materials showed a superior electrochemical behavior in Li-O_2 battery. Due to that, the catalyst nanoparticles were uniformly dispersed over the high surface area carbon support, and that the porous structure and surface area were well persevered by the catalysts deposition methods used in this protocol. The overall reaction of nonaqueous Li-O_2 battery is $2Li^+ + O_2 + 2e^- \rightarrow Li_2O_2$.[2,3,7] Side reactions, such as electrolyte decomposition, are also likely to occur due to the activity of the materials and intermediates used in a cell. However, in the research at the present stage, the side reactions and byproducts (LiOH, Li_2CO_3, *etc.*) have been significantly reduced with the improvement of materials and synthesis technologies. As shown in **Figure 2d**, although there might be a small amount of byproducts, the amount is too low to be detected by XRD. Some surface-sensitive techniques, such as XPS, FT-IR, and Raman spectroscopy, are, therefore, used to detect the minor products, especially on the surface region. There is no doubt that the stability of the electrolytes is very critical in oxygen environment and electrochemical reactions. Ether-based electrolytes (*e.g.*, TEGDME) are relatively stable at the present stage of Li-O_2 battery research. However, their behavior still needs to be investigated during long-term cycling; and searching for stable electrolytes is the research priority presently.

There are some other characterization methods to establish the discharge yield, or byproducts, such as mass spectrometry (MS) and titration. However, in the current research stage, the battery system is much more stable and reversible, and the byproducts have been significantly reduced by the development of electrolyte and cathode materials which have been more stable to oxygen and the discharge products.[3,13,15] In this case, MS and titration are not sensitive enough to estimate the discharge yield. Besides, LiO_2, the intermediate product, cannot be detected by titration either, due to its extreme activity.

In this article, we have demonstrated a systematic and efficient protocol of routine tests of aprotic Li-O_2 battery, including the performance test and characterization of battery materials and reaction products. The approaches of catalyst loading result in a uniform distribution of catalyst nanoparticles with preservation of the surface structure of carbon substrate. Appropriate assembly protocol optimizes the active materials and ensures the pure-O_2 environment for the electrochemical reactions.

Disclosures

The authors have nothing to disclose.

Acknowledgements

Research at Argonne National Laboratory was funded by U.S. Department of Energy, FreedomCAR and Vehicle Technologies Office. Use of the Advanced Photon Source and research carried out in the Electron Microscopy Center at Argonne National Laboratory was supported by the U.S. Department of Energy, Office of Science, Office of Basic Energy Sciences, under Contract No. DE-AC02-06CH11357.

References

1. Abraham, K. M., & Jiang, Z. A polymer electrolyte-based rechargeable lithium/oxygen battery. *J. Electrochem. Soc.* **143**, 1-5 (1996).
2. Bruce, P. G., Freunberger, S. A., Hardwick, L. J., & Tarascon, J.-M. Li-O_2 and Li-S batteries with high energy storage. *Nat. Mater.* **11**, 19-29 (2012).
3. Lu, J. *et al.* Aprotic and Aqueous Li-O_2 Batteries. *Chem. Rev.* **114**, 5611-5640 (2014).
4. Black, R., Adams, B., & Nazar, L. F. Non-Aqueous and Hybrid Li-O_2 Batteries. *Adv. Energy Mater.* **2**, 801-815 (2012).
5. Bruce, P. G., Hardwick, L. J., & Abraham, K. M. Lithium-air and lithium-sulfur batteries. *MRS Bull.* **36**, 506-512 (2011).
6. Christensen, J. *et al.* A Critical Review of Li/Air Batteries. *J. Electrochem. Soc.* **159**, R1-R30 (2012).
7. Girishkumar, G., McCloskey, B., Luntz, A. C., Swanson, S., & Wilcke, W. Lithium-Air Battery: Promise and Challenges. *J. Phys. Chem. Lett.* **1**, 2193-2203 (2010).
8. Lu, J., & Amine, K. Recent Research Progress on Non-aqueous Lithium-Air Batteries from Argonne National Laboratory. *Energies.* **6**, 6016-6044 (2013).
9. Ding, N. *et al.* Influence of carbon pore size on the discharge capacity of Li-O2 batteries. *J. Mater. Chem. A* **2**, 12433 (2014).
10. Nimon, V. Y., Visco, S. J., De Jonghe, L. C., Volfkovich, Y. M., & Bograchev, D. A. Modeling and Experimental Study of Porous Carbon Cathodes in Li-O2 Cells with Non-Aqueous Electrolyte. *ECS Electrochem. Lett.* **2**, A33-A35 (2013).
11. Ottakam Thotiyl, M. M., Freunberger, S. A., Peng, Z., & Bruce, P. G. The Carbon Electrode in Nonaqueous Li-O_2 Cells. *J. Am. Chem. Soc.* **135**, 494-500 (2012).
12. Park, J.-B., Lee, J., Yoon, C. S., & Sun, Y.-K. Ordered Mesoporous Carbon Electrodes for Li-O2 Batteries. *Acs Appl. Mater. Interfaces.* **5**, 13426-13431 (2013).
13. Lei, Y. *et al.* Synthesis of porous carbon supported palladium nanoparticle catalysts by atomic layer deposition: application for rechargeable lithium-O2 battery. *Nano Lett.* **13**, 4182-4189 (2013).
14. Lu, J. *et al.* Effect of the size-selective silver clusters on lithium peroxide morphology in lithium-oxygen batteries. *Nat. Commun.* **5,** 4895 (2014).
15. Lu, J. *et al.* A nanostructured cathode architecture for low charge overpotential in lithium-oxygen batteries. *Nat. Commun.* **4,** 2383 (2013).
16. Lu, J. *et al.* Synthesis and characterization of uniformly dispersed Fe_3O_4/Fe nanocomposite on porous carbon: application for rechargeable Li-O_2 batteries. *RSC Adv.* **3**, 8276-8285 (2013).
17. Luo, X. *et al.* Pd nanoparticles on ZnO-passivated porous carbon by atomic layer deposition: an effective electrochemical catalyst for Li-O_2 battery. *Nanotechnology* **26**, 164003 (2015).
18. Freunberger, S. A. *et al.* The Lithium-Oxygen Battery with Ether-Based Electrolytes. *Angew. Chem. Int. Ed.* **50**, 8609-8613 (2011).

19. Laoire, C. O., Mukerjee, S., Abraham, K. M., Plichta, E. J., & Hendrickson, M. A. Influence of Nonaqueous Solvents on the Electrochemistry of Oxygen in the Rechargeable Lithium-Air Battery. *J. Phys. Chem. C.* **114**, 9178-9186 (2010).
20. McCloskey, B. D., Bethune, D. S., Shelby, R. M., Girishkumar, G., & Luntz, A. C. Solvents' Critical Rope in Nonaqueous Lithium-Oxygen Battery Electrochemistry. *J. Phys. Chem. Lett.* **2**, 1161-1166 (2011).
21. Assary, R. S. *et al.* Molecular-Level Insights into the Reactivity of Siloxane-Based Electrolytes at a Lithium-Metal Anode. *ChemPhysChem* **15**, 2077-2083 (2014).
22. Du, P. *et al.* Compatibility of lithium salts with solvent of the non-aqueous electrolyte in Li-O_2 batteries. *Phys. Chem. Chem. Phys.* **15**, 5572-5581 (2013).
23. Aleshin, G. Y. *et al.* Protected anodes for lithium-air batteries. *Solid State Ion.* **184**, 62-64 (2011).
24. Assary, R. S. *et al.* The Effect of Oxygen Crossover on the Anode of a Li-O_2 Battery using an Ether-Based Solvent: Insights from Experimental and Computational Studies. *ChemSusChem* **6**, 51-55 (2013).
25. Aurbach, D., Zinigrad, E., Cohen, Y., & Teller, H. A short review of failure mechanisms of lithium metal and lithiated graphite anodes in liquid electrolyte solutions. *Solid State Ion.* **148**, 405-416 (2002).
26. Dey, A. N. Lithium Anode Film And Organic And Inorganic Electrolyte Batteries. *Thin Solid Films.* **43**, 131-171 (1977).
27. Lau, K. C., Lu, J., Luo, X., Curtiss, L. A., & Amine, K. Implications of the Unpaired Spins in Li-O_2 Battery Chemistry and Electrochemistry: A Minireview. *ChemPlusChem.* **80**, 336-343 (2015).
28. Lau, K. C. *et al.* Theoretical Exploration of Various Lithium Peroxide Crystal Structures in a Li-Air Battery. *Energies* **8**, 529-548 (2015).
29. Black, R. *et al.* Screening for Superoxide Reactivity in Li-O_2 Batteries: Effect on Li_2O_2/LiOH Crystallization. *J. Am. Chem. Soc.* **134**, 2902-2905 (2012).
30. Gallant, B. M. *et al.* Influence of Li_2O_2 morphology on oxygen reduction and evolution kinetics in Li-O_2 batteries. *Energy Environ. Sci.* **6**, 2518-2528 (2013).
31. Lu, J. *et al.* Magnetism in Lithium-Oxygen Discharge Product. *ChemSusChem* **6**, 1196-1202 (2013).
32. Xu, J.-J., Wang, Z.-L., Xu, D., Zhang, L.-L., & Zhang, X.-B. Tailoring deposition and morphology of discharge products towards high-rate and long-life lithium-oxygen batteries. *Nat. Commun.* **4**, 2438 (2013).
33. Zhong, L. *et al.* In Situ Transmission Electron Microscopy Observations of Electrochemical Oxidation of Li_2O_2. *Nano Lett.* **13**, 2209-2214 (2013).
34. *Hitachi S-4700 SEM Training & Reference Guide.* <http://chanl.unc.edu/files/2013/04/sem-user-guide_v1.pdf> (2015).
35. *Hitachi S4700 User Manual.* <http://www.toyota-ti.ac.jp/Lab/Material/surface/naibu/SEM%20Hitachi%20S4700%20User%20Manual.doc.> (2015).
36. Goldstein, J. *et al. Scanning Electron Microscopy and X-ray Microanalysis.* Springer: New York, NY (2003).
37. *Ray Photoelectron Spectrometer Operation Procedure.* <https://nanofabrication.4dlabs.ca/uploads/documents/XPS_SOP.pdf> (2015).
38. Haasch, R. T. in *Practical Materials Characterization.* (ed Mauro Sardela) Ch. 3, 93-132, Springer: New York, NY (2014).
39. *Field Emission Transmission Electron Microscope.* <http://cmrf.research.uiowa.edu/files/cmrf.research.uiowa.edu/files/JEOL%202100%20User%20Instructions.pdf> (2015).
40. Wen, J.-G. in *Practical Materials Characterization.* (ed Mauro Sardela) Ch. 5, 189-229, Springer: New York, NY (2014).
41. Williams, D. B., & Carter, C. B. *Transmission Electron Microscopy.* Springer: New York, NY (2009).
42. *Beamline 11-ID-C: High-energy Diffraction Beamline.* <http://www.aps.anl.gov/Beamlines/Directory/showbeamline.php?beamline_id=15> (2015).
43. *Beamline 11-ID-D: Sector 11 - Time Resolved X-ray Spectroscopy and Scattering.* <http://www.aps.anl.gov/Beamlines/Directory/showbeamline.php?beamline_id=17> (2015).
44. Sardela, M. R. in *Practical Materials Characterization.* (ed Mauro Sardela) Ch. 1, 1-41, Springer: New York, NY (2014).
45. *Beamline 9-BM-B,C: X-ray Absorption Spectroscopy Beamline.* <http://www.aps.anl.gov/Beamlines/Directory/showbeamline.php?beamline_id=82> (2015).
46. *Beamline 20-BM-B: X-ray Absorption Spectroscopy Beamline.* <http://www.aps.anl.gov/Beamlines/Directory/showbeamline.php?beamline_id=32> (2015).
47. Bunker, G. *Introduction to XAFS: A Practical Guide to X-ray Absorption Fine Structure Spectroscopy.* Cambridge University Press, 1st edition. (2010).
48. *Nicolet FT-IR User's Guide.* <http://chemistry.unt.edu/~verbeck/LIMS/Manuals/6700_User.pdf> (2015).
49. *Nicolet iS5 User Guide.* <http://madisonsupport.thermofisher.com/Molecular&UV8/Nicolet%20iS5%20User%20Guide.pdf> (2015).
50. *Renishaw inVia Raman Microscope Training Notebook.* <https://depts.washington.edu/ntuf/facility/docs/raman_training_rev2_120507.pdf> (2015).
51. *Renishaw InVia Quick Operation Summary.* <https://www.ccmr.cornell.edu/sites/default/files/facilities%20equipment/Raman_Operation_Procedures_July_14_2014.pdf> (2015).
52. Mitchell, R. R., Gallant, B. M., Thompson, C. V., & Shao-Horn, Y. All-carbon-nanofiber electrodes for high-energy rechargeable Li-O_2 batteries. *Energy Environ. Sci.* **4**, 2952-2958 (2011).

